Magnetic structure of TbD_2—A neutron diffraction study*

H. Shaked,† J. Faber Jr., M. H. Mueller, and D. G. Westlake
Argonne National Laboratory, Argonne, Illinois 60439
(Received 22 March 1977)

Terbium dideuteride has been examined by elastic neutron scattering. Crystallographic parameters have been determined at 300 and 77 K. It was found that TbD_2 undergoes a para- to antiferromagnetic transition at $T_N = 17.2(3)$ K. The magnetic structure at 4.6 K was determined and found to belong to the monoclinic space group $C_{2c}2/m'$. The magnetic moment per Tb^{3+} ion is 7.6(3) μ_B at 4.6 K. The reduction from the free-ion value of 9.0 μ_B/Tb^{3+} is due to crystalline electric field effects that are also apparent in the temperature dependence of the sublattice magnetization.

I. INTRODUCTION

The rare earths form hydrides that have been the subject of many studies.[1-3] Considerable interest was rejuvenated in these hydrides in the last few years relative to hydrogen and energy storage (solar converters) materials. The dihydrides, MH_2, crystallize in the cubic fluorite sturcture[1] and have a finite range of stable compositions that encompasses the H/M ratio of 2.[4] They have metallic conduction[3] and most undergo a transition to magnetic order at low temperature.[2] The fluorite structure has octahedral and tetrahedral sites that are occupied by M and H, respectively (Fig. 1). However, an additional octahedral site is generally vacant, but as the H/M ratio exceeds 2, the excess H goes into this vacant site. Some workers have reported[5] a few percent of H in this "vacant" site in $CeD_{1.98}$, whereas others have reported[6] that this octahedral site was vacant in $CeD_{2.00}$. This point will be discussed in characterizing our TbD_2 sample.

Dihydrides that exhibit magnetic ordering are ferromagnetic with Eu or lighter rare earths and antiferromagnetic with Tb or heavier rare earths.[2] According to early reports[7] based on studies of the magnetic susceptibility of TbH_x ($x \sim 2$), T_N was ~40 K. In a neutron diffraction study that followed,[8] a modulated magnetic structure was proposed on the basis of a 4.2-K pattern with unusually broad magnetic reflections and a poor agreement with calculated intensities. The proposed magnetic structure was not commensurate with the crystallographic lattice. In recent specific-heat and magnetic-susceptibility studies[9] of $TbH_{2.01}$, it was found that $T_N \sim 17$ K. In the present work, we find that the magnetic structure of TbD_2 is commensurate with the crystallographic lattice and has $T_N \sim 17.2$ K.

A different, but somewhat related question of fundamental interest in the rare-earth hydrides, concerns the charge of the hydrogen ion, namely, whether it is negative (hydridic) or positive (protonic). The hydridic model will, in general, lead to a crystalline electric-field (CEF) ground state for the Tb^{3+} ion that is different from the CEF ground state of the protonic model. Because the saturated sublattice magnetization (henceforth called magnetic moment) is related to the ground state of Tb^{3+} in the crystal, it may be possible to determine which of the two models is valid in TbD_2. We will consider this question in Sec. V.

II. EXPERIMENT

A terbium ingot, purity given as 99.9%, was obtained from Alfa Products, Danvers, Mass. 18 g of terbium were placed in a tube made of molybdenum foil and inserted in a modified Sieverts apparatus. The pressure was reduced to 2.7×10^{-4} Pa before the specimen was heated to 1075 K. This step was taken to remove protium (^1H); however, the specimen was found to contain virtually none. Deuterium was generated by thermal decomposition of UD_3. A mass spectrometric analysis of the deuterium gas revealed only 0.4% protium. The specimen was charged with deuterium in four

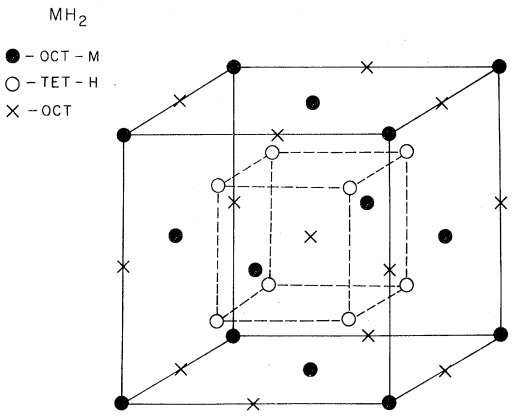

FIG. 1. Crystallographic unit cell (fluorite structure) of metal dihydrides.

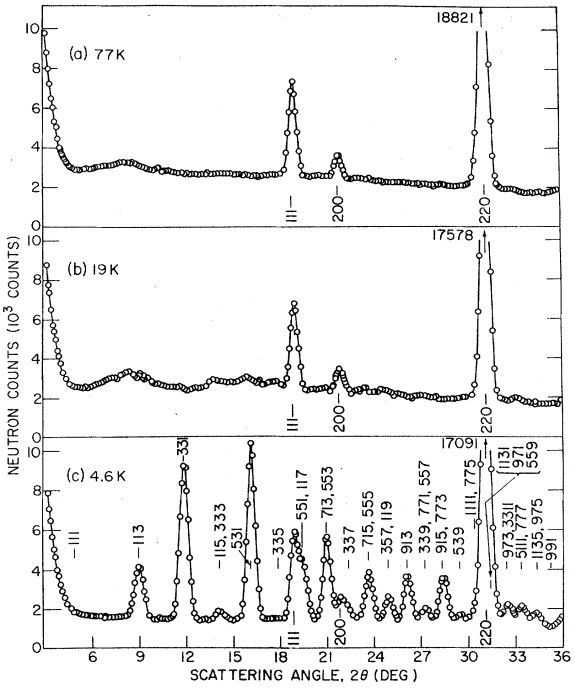

FIG. 2. Neutron diffraction patterns of polycrystalline TbD_2 at (a) 77 K, (b) 19 K, (c) 4.6 K. The nuclear lines are indexed (bottom) according to $a_0 = 5.219$ Å. The magnetic lines are indexed according to $4a_0$.

steps. It was allowed to react at 1075 K with D_2 at a pressure of $<5 \times 10^3$ Pa until the atom fraction D/Tb = 0.7. The sample was cooled to room temperature, additional D_2 was generated, and the charging step was repeated. At the end of the final step, the temperature was reduced to 998 K and an equilibrium pressure of 400 Pa resulted. After all experiments were completed, 0.1 g of the deuteride specimen was analyzed by vacuum extraction at 1075 K, and the atom fraction was found to be D/Tb = 1.93(2).

The deuterated specimen (15.3 g) was crushed and loaded under argon atmosphere into a cylindrical vanadium cell (11 mm in diameter and 35 mm long). A neutron beam ($\lambda = 0.991$ Å) was obtained from a Ge(311) monochromator in transmission. Wavelength contamination ($\frac{1}{2}\lambda, \frac{1}{3}\lambda$) was <0.01%.

TABLE I. Lattice constants and thermal parameters for TbD_2. The scattering amplitudes used in the refinements were (Ref. 10) 0.667 and 0.76 (10^{-12} cm) for D and Tb, respectively.

Temperature (°K)	a_o (Å)	B (Å²) [a] D	Tb	R(%) [b]
300	5.233(2)	1.33(5)	0.47(4)	1.5
77	5.219(2)	0.74(5)	0.11(5)	2.0

[a] An absorption correction (Ref. 11) of 0.03 was added to the refined values.

[b] Weighted R factor is $\{\sum[(F^2_{obs}-F^2_{calc})^2/\sigma]/(F^2_{obs}/\sigma)^2\}^{1/2}$.

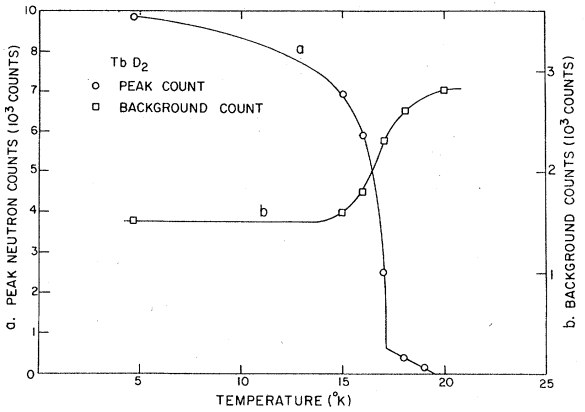

FIG. 3. Temperature dependence of (a) peak count of {531} and (b) background count. The solid lines are visual guides.

III. RESULTS

Neutron diffraction patterns were obtained (Fig. 2) at 4.6, 19, 77, and 300 K (not shown in figure). Many new reflections appeared when the specimen was cooled to 4.6 K. The temperature dependence of one of these reflections (Fig. 3) indicates a transition at 17.2(3) K, which is in agreement with the temperature for the antiferromagnetic transition in $TbD_{2.01}$.[9] Thus, these new reflections are magnetic in origin. They cannot be indexed in terms of the crystallographic lattice constant a_0 (Table I). If we consider only magnetic unit cells, the edges of which are integral multiples of a_0, then the dimensions of the smallest rectangular unit cell that permits indexing of the magnetic lines are $4a_0 \times 4a_0 \times 4a_0$.

The decrease in background (Fig. 3), as the specimen is cooled through T_N, is due to the disappearance of the paramagnetic scattering. The results shown in Fig. 3 were derived from the scans shown in Fig. 4. As the specimen is cooled through T_N, a line at $2\theta = 17.5°$ appears (see 17 and 18 K) that cannot be indexed according to the magnetic unit cell. The line disappears as the sample is cooled 3 to 4 K below T_N. This phenomenon may be related to the transition, but, at present, we have no suitable explanation. The broad "line" at about $2\theta \sim 8°$ in the 77 K pattern is probably due to magnetic short-range order [Fig. 2(a)]. This "line," although significantly diminished, is still apparent at 300 K.

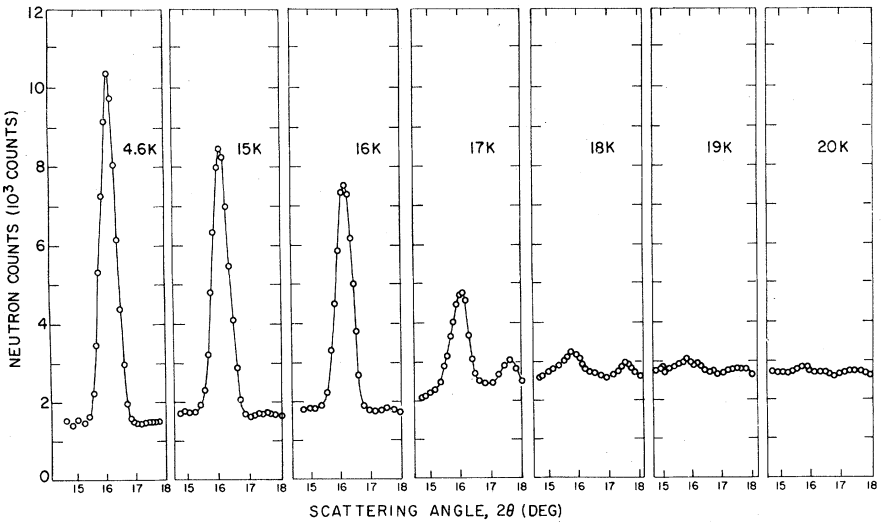

FIG. 4. 2θ scans of the $\{531\}$ reflection at several temperatures above and below T_N.

IV. ANALYSIS

A. Crystallography

Neutron reflections up to and including $\{800\}$ were obtained and indexed according to the lattice constants given in Table I. Eighteen distinct lines were present in each pattern. Least-squares refinements of x (in TbD_x) and the isotropic temperature factors of Tb and D, with respect to the integrated intensities, were performed for the patterns obtained at 77 and 300 K. These refinements yielded $x = 1.96 (R = 1.5\%)$, and $2.01 (R = 2.0\%)$ for the 300 and 77 K patterns, respectively. Additional refinements were attempted for which the deuterium was allowed to occupy the vacant octahedral site. Although results indicated that 1% and 2% of the deuterium could occupy the octahedral site at 300 and 77 K, respectively, a larger discrepancy in x between the two patterns and unusually large (~8 Å^2) temperature factors were obtained. Hence, x was set at 1.98(4), and a third refinement (with the deuterium excluded from the octahedral site) was performed. The results are presented in Table I. The temperature factors at 300 K compare well with 1.44(3) and 0.44(5) Å^2 that were reported[6] for $CeD_{2.00}$.

B. Magnetic structure

The search for a magentic structure, consistent with the pattern observed at 4.6 K, was restricted to "nonmodulated" collinear structures. This restriction is justified *a posteriori* by our solution of the structure, but was also reasonable *a priori* because ErH_2 (Ref. 12) and HoD_2 (Ref. 13) have nonmodulated structures. We thus use the standard formula for the integrated intensity[11]

$$I(G) \propto j(G) q(G)^2 f(G)^2 |F(G)|^2 p^2 \mathrm{LP}(G) , \tag{1}$$

where

$$j(G) q(G)^2 |F(G)|^2 = \sum_{\vec{G}} q(\vec{G})^2 |F(\vec{G})|^2 ,$$

$$\vec{G} = \vec{G}_1 \cdots \vec{G}_j \tag{2}$$

and

$$F(\vec{G}) = \sum_{\vec{R}} s(\vec{R}) e^{i\vec{G}\cdot\vec{R}} . \tag{3}$$

We use, for the reciprocal-lattice and position vectors,

$$\vec{G} = (2\pi/a)(h[100] + k[010] + l[001]) \tag{4}$$

and

$$\vec{R} = \tfrac{1}{8} a (n[110] + m[011] + t[101]) , \tag{5}$$

respectively. The summations are over all $\vec{G}$ for which $|\vec{G}| = G$ and over all $\vec{R}$ in the magnetic unit cell, $|s(\vec{R})| = 1$ and the sign of $s(\vec{R})$ is determined by the direction of the magnetic moment at $\vec{R}$, and $\mathrm{LP}(G)$ is the Lorenz-polarization factor. It has been established that (i) the observed pattern is indexed on a lattice defined by $a[100]$, $a[010]$, $a[001]$ where $a = 4a_0$, and (ii) the observed reflections are all odd.

It will be shown that these results are sufficient to impose some useful constraints on the $\vec{G}$ dependence of $F(\vec{G})$. From Eqs. (3)–(5)

$$F(h,k,l) = \sum_{n,m,t} s(n,m,t) \exp\{\tfrac{1}{4}\pi i[(h+k)n + (k+l)m + (h+l)t]\} . \tag{6}$$

Hence,

TABLE II. Calculation of the observed form factor (last column) from the observed intensities (second column).

$\{hkl\}$ [a]	I(obs)	LP [b]	jq^2	$0.037\,82\,[I/(\mathrm{LP}jq^2)]^{1/2}$
111	0(150)	...	...	...
131	18 976(250)	161.93	0.1818	0.960(9)
313	53 205(310)	93.96	0.9474	0.925(3)
333, 151	2 799(170)	66.27	0.0740	0.903(24)
315	54 056(320)	51.24	1.9428	0.882(4)
533	0(150)	...	...	...
171, 515	17 280(720)	35.33	0.9804	0.846(22)
535, 137	25 200(720)	30.61	1.6950	0.834(15)
373	Obscured	...	...	...
555, 751	15 120(480)	24.19	1.3333	0.820(13)
911, 573	8 064(480)	21.91	0.8192	0.803(24)
931	16 130(720)	20.03	1.8022	0.800(11)
771, 393, 575	4 555(480)	18.46	0.6894	0.717(41)
159, 737	16 130(720)	17.12	2.4479	0.742(17)
395	2 400(480)	15.97	0.4174	0.717(76)
757, $1\mathring{1}1$	Obscured	...	...	...
197, $31\mathring{1}$, 595	Obscured	...	...	...
$33\mathring{1}$, 937	8 064(1,200)	13.31	1.8706	0.681(52)
777, $\mathring{1}15$	7 680(1,200)	12.61	1.9864	0.662(53)
$\mathring{1}53$, 759	6 000(1,200)	11.99	1.6774	0.654(69)
199	0(300)	...	...	...

[a] $hk\mathring{l}$ means that 10 should be added to l, for example $\mathring{3}37 = 13\,3\,7$.
[b] LP is the Lorenz-polarization factor, $\mathrm{LP} = (\sin\theta\,\sin 2\theta)^{-1}$.

$$F(h,k,l) = F(h\pm 8,k,l) = F(h,k\pm 8,l) = F(h,k,l\pm 8) = F(h\pm 4,k+4,l\pm 4). \quad (7)$$

It follows that, for any odd, odd, odd reflection, $F(h,k,l)$ is equal to either $F(\vec{G}_1)$ or $F(\vec{G}_2)$, where $\vec{G}_1$ and $\vec{G}_2$ belong to the forms $\{111\}$ and $\{131\}$, respectively.

We now make two simplifying assumptions (a) Since $I(\mathrm{obs}) = 0$ for $\{111\}$, then $F(\vec{G}_1) = 0$ for all $\vec{G}_1$. It follows that $F(h,k,l) = 0$ for all reflections related to $\{111\}$ through Eq. (7), e.g., $\{333\}$, $\{117\}$. Note that $\{335\}$ is indeed not observed (Fig. 2); and (b) $F(\vec{G}_2) \neq 0$ only for a single member of the $\{131\}$ form, say $(13\bar{1})$. This leads to a tremendous simplification, such that the validity of the assumptions can be tested without solving for the structure. Since the nonzero $|F(G)|$'s are now independent of G, we can set $I(G) = I(\mathrm{obs})$ in Eq. (1) and solve for $f(G)$. Using $F(13\bar{1}) \neq 0$, we have solved for $f(G)$ with the antiferromagnetic axis along the 13 symmetrical directions (three $\langle 100\rangle$, four $\langle 111\rangle$, and six $\langle 101\rangle$). Only [010] yielded a smooth dependence of f on $\sin\theta/\lambda$ ($\sin\theta/\lambda = G/4\pi$). The calculations for this direction are given in Table II, and the resultant form factor f is shown in Fig. 5. The good agreement with other experimental and theoretical results demonstrates the good quality of the data and the validity of the above simplifications. We conclude that (i) $F(G) = 0$ for all members of $\{111\}$; (ii) $F(G) = 0$ for all members of $\{131\}$ *except* $(13\bar{1})$; and (iii) the antiferromagnetic axis is along [010].

Our next step is to find an $s(\vec{R})$ that will satisfy conclusion (i). The primitive reduced magnetic unit cell[15] (PRMUC) contains 32 magnetic ions. The number of possible collinear structures is immense. If we require that the PRMUC be antiferromagnetic, then we still have $\frac{1}{2}C(32,16) \sim 3\times 10^8$ structures to investigate. Fortunately, this is not required. It is reasonable to expect that a motif smaller than 32 ions exists, which is repeated through translations and/or antitranslations. In other words, the real PRMUC is smaller than $2a_0 \times 2a_0 \times 2a_0$. Writing down the structure factor, we were able to find a motif of two ions with

$$\vec{R} = 0,0,0;\ -\tfrac{1}{2},\tfrac{1}{2},0, \qquad s(\vec{R}) = +1;\ -1. \quad (8)$$

This motif with a translation $a_0[\frac{1}{2}\frac{1}{2}0]'$ (the prime designates an antitranslation) satisfied conclusion (i). Furthermore, given the translations $a_0[\bar{1}10]'$, $a_0[\frac{1}{2}0\frac{1}{2}]$, and the previous translation, conclusion (ii) is satisfied. The solution is complete. The structure and the lattice are illustrated in Fig. 6.

The magnitude of the magnetic moment (in Bohr magnetons) is given by $n_B = p/0.27$, where p (in

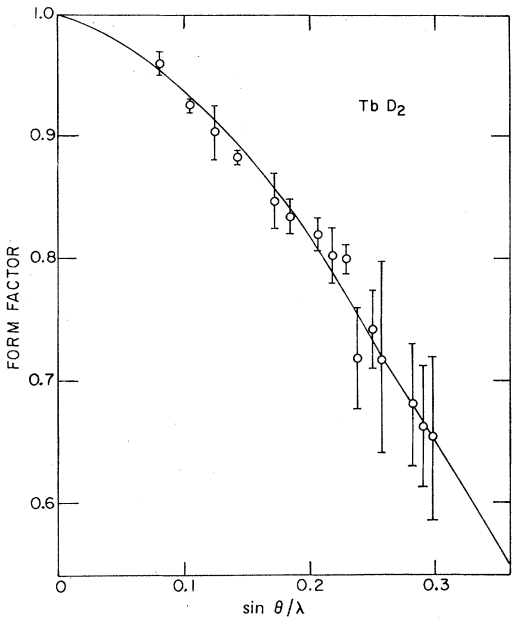

FIG. 5. Magnetic form factor of Tb^{3+} as calculated from I(obs) of TbD_2. The solid line represents results obtained (Ref. 14) with $Tb(OH)_3$. The TbD_2 results were scaled so that the first two reflections fit the solid line. Note that the ordinate begins at $f = 0.55$.

units of 10^{-12} cm) is calculated from the expression

$$p^2 = \frac{j_N}{j_M q^2} \frac{F_N^2}{F_M^2} \frac{(\mathrm{LP})_N}{(\mathrm{LP})_M} \frac{1}{f_M^2} \frac{I(\mathrm{obs})_M}{I(\mathrm{obs})_N}. \quad (9)$$

Magnetic and nuclear quantities are given subscripts M and N, respectively. The structure factors are given by

$$F_M = 4[1 - e^{\pi i(-h+k)/4}][1 - e^{\pi i(h+k)/4}] \times [1 + e^{\pi i(h+k)/2}][1 + e^{\pi i(h+l)/4}] \times [1 + e^{\pi i(h+l)/2}][1 - e^{\pi i(-h+k)/2}] \quad (10)$$

and

$$F_N = 256[b_{\mathrm{Tb}} + 2b_{\mathrm{D}} \cos\tfrac{1}{8}\pi(h+k+l)]. \quad (11)$$

Taking {531} and {444} ({111} in the crystallographic unit cell) for M and N, respectively, we obtain $n_B = 7.6(3)\mu_B$.

V. DISCUSSION

The magnetic structure has mirror symmetry about the (101) atomic planes (Fig. 6). The PRMUC of Fig. 6, although the smallest cell, is of triclinic symmetry and does not exhibit this symmetry of the magnetic structure. It is therefore convenient to project the structure onto the (101) plane (Fig. 7). With this projection, it is apparent that the structure has a twofold axis along [101]. The standard monoclinic lattice[16] [indicated by the monoclinic cell in Fig. 7(a)] is C_{2c} and the space group is $C_{2c}2/m'$. The volume of the base-center-reduced monoclinic magnetic unit cell [Fig. 7(b)] is a_0^3 (where a_0 is the crystallographic lattice constant). The smallest rectangular reduced cell [Fig. 7(a)] has a volume of $2a_0^3$. The structure consists of pairs of ferromagnetic $(13\bar{1})$ planes coupled antiferromagnetically. It has a propagation vector along $[13\bar{1}]$ of length $\sqrt{\frac{3}{2}}a_0$, and the structure is reminiscent of Ia-type ordering in a fcc lattice. The reduction in symmetry from $Fm3m1'$ in the paramagnetic state to $C_{2c}2/m'$ in the antiferromagnetic state is $2 \times \frac{192}{8} = 48$-fold. Hence, we have 48 domains.

As the specimen is cooled below T_N, the sublattice magnetization, which is proportional to the square root of the peak count (Fig. 3), increases more rapidly than would be predicted for the free ion by molecular-field theory (Brillouin curve with $J = 6$). This is due to the strong CEF, which is also responsible for the reduction in the magnetic moment (at 4.6 K) from 9 (free ion) to $7.6\mu_B$.

The Tb^{3+} ion has six unpaired $4f$ electrons and the Russell-Saunders Hund's-rule ground state is $^7F_6$. This state is split primarily by the CEF due to the eight nearest-neighbor deuterium ions (Fig.

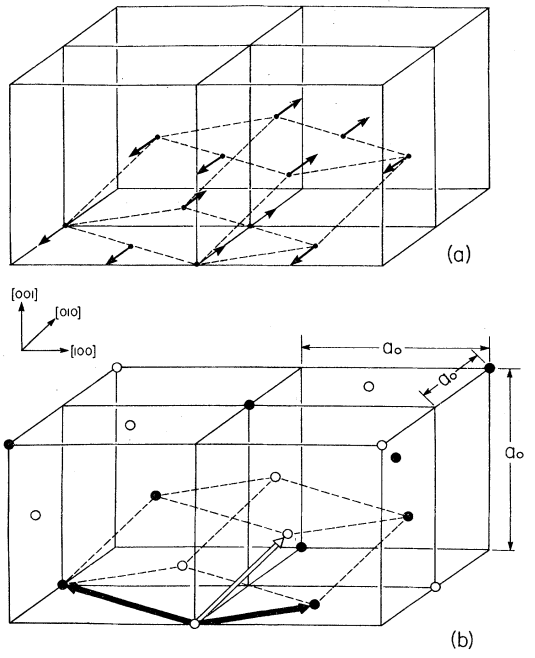

FIG. 6. Proposed magnetic structure of TbD_2 at 4.6 K. (a) The magnetic structure. The moments are directed along [010]. (b) The magnetic lattice. In (b), light and dark arrows represent translations and antitranslations, respectively. The dashed lines show the triclinic PRMUC.

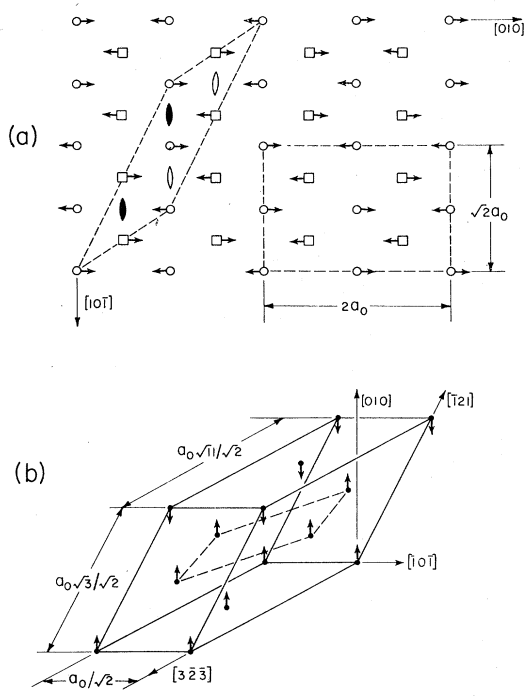

FIG. 7. (a) (101) projection of the magnetic structure. The squares are in a plane shifted from the plane of the circles by $a_0/(2\sqrt{2})$—half a lattice translation along [101]. The standard monoclinic and the smallest rectangular reduced cells are indicated by dashed lines. The light and dark twofold symbols designate 2 and 2′ axes, respectively. (b) The standard monoclinic, base-centered-reduced unit cell for the C_{2c} lattice.

1). The ground-CEF level can be Γ_2 or Γ_3 in the hydridic model, and $\Gamma_5^{(1)}$ or Γ_1 in the protonic model.[17] A magnetic ground state was ruled out by Mössbauer experiments[18]; therefore, we consider the three nonmagnetic states Γ_1, Γ_2, and Γ_3, where the exchange field induces a magnetic moment analogous to that obtained in Van Vleck paramagnetism. Assuming that only matrix elements between the ground state and one-excited state are important[19] (weak magnetic field), the magnetic moments are bound (see Appendix) by $g[J(J+1)/3]^{1/2} = 5.61\mu_B$ and $g[J(J+1)2/3]^{1/2} = 7.9\mu_B$ in the case of singlet and doublet ground states, respectively. Within this approximation, Γ_1 as a ground state cannot produce the observed magnetic moment of $7.6\mu_B$. If the magnetic field, on the other hand, is sufficiently strong, the approximation breaks down and this system can produce $7.6\mu_B$ through admixing $\Gamma_5^{(1)}$ into Γ_1 via Γ_4. However, in the latter case it was shown[20] that the easy direction of magnetization is along [111] which is in disagreement with the observed [010] direction of magnetic moment. Hence, Γ_1 as a ground state is inconsistent with either the magnitude (weak field) or direction (strong field) of the observed magnetic moment. This result is consistent with the hydridic model found in other rare-earth hydrides.[12]

VI. SUMMARY

It was found that TbD_2 exhibited a para- to antiferrogmagnetic transition at $T_N = 17.2(3)$ K. The magnetic structure at 4.6 K was determined and found to belong to the monoclinic space group $C_{2c}2/m'$. The magnetic moment at 4.6 K is $7.6(3)\mu_B$. The latter result and the Mössbauer experimental results require that the CEF ground state is Γ_3, which corresponds to the hydridic model. Information about the ground level as well as excited levels of Tb^{+3} in TbD_2 may be obtained from inelastic neutron scattering. It is felt that such an experiment is warranted.

ACKNOWLEDGMENTS

The authors are grateful to R. L. Hitterman and J. F. Reddy for technical assistance and to G. K. Shenoy, B. D. Dunlap, D. J. Lam, and B. R. Cooper for useful discussions.

APPENDIX

An upper limit of the magnetic moment

$$\mu \leq g[NJ(J+1)/3]^{1/2},$$

where $N = 1$, 2, and 3 for a singlet, doublet and triplet, respectively, can be obtained using the following property of Hermitian matrices:

$$\sum_{\Gamma,\Gamma'} |\langle \Gamma | J_z | \Gamma' \rangle|^2 = \sum_{-J}^{J} M^2 = \frac{2J+1}{3} J(J+1).$$

The sum rule (for intensities) asserts[21] that the sum of intensities of the multiplet components with a common initial state is proportional to the *a priori* probability of the common initial state, which is the degeneracy, N_Γ. Hence we have

$$\sum_{\Gamma'} |\langle \Gamma | J_z | \Gamma' \rangle|^2 = \tfrac{1}{3} N_\Gamma J(J+1).$$

*Work supported by the U. S. ERDA.

†On leave from the Nuclear Research Center, Negev, and Ben-Gurion University, Negev, Beer Sheva, Israel.

[1] W. G. Bos and K. H. Gayer, J. Nucl. Mater. 18, 1 (1960).
[2] W. E. Wallace, Ber. Bunsen-Gesell. 76, 832 (1972).
[3] G. G. Libowitz, Ber. Bunsen-Gesell. 76, 837 (1972).

[4]A. Pebler and W. E. Wallace, J. Phys. Chem. 66, 148 (1962).
[5]P. Vorderwisch and S. Hautecler, Phys. Status Solidi B 66, 595 (1974).
[6]A. K. Cheetham and B. E. F. Fender, J. Phys. C 5, L35 (1972).
[7]W. E. Wallace, Y. Kubota, and R. L. Zanowick, Adv. Chem. 39, 122 (1963).
[8]D. E. Cox, G. Shirane, W. J. Takei, and W. E. Wallace, J. Appl. Phys. 34, 1352 (1963).
[9]Z. Bieganski, J. Opyrchal, and M. Drulis, Solid State Commun. 17, 353 (1975).
[10]Neutron Diffraction Commission, Acta Crystallogr. A 28, 357 (1972).
[11]G. E. Bacon, *Neutron Diffraction* (Clarendon, Oxford, 1962), pp. 97 and 163.
[12]G. K. Shenoy, B. D. Dunlap, D. G. Westlake, and A. E. Dwight, Phys. Rev. B 14, 141 (1976).
[13]G. K. Shenoy and B. D. Dunlap (private communication).
[14]G. H. Lander, T. O. Brun, J. P. Desclaux, and A. J. Freeman, Phys. Rev. Lett. 8, 3237 (1973).
[15]The PRMUC is the smallest unit cell formed by the magnetic lattice ($2a_0 \times 2a_0 \times 2a_0$ in this case) and is therefore smaller than the primitive magnetic unit cell when the magnetic lattice contains antitranslations.
[16]W. Opechowski and R. Guccione, in *Magnetism*, edited by G. T. Rado and H. Suhl (Academic, New York, 1965), Vol. IIa.
[17]K. R. Lea, M. J. M. Leask, and W. O. Wolf, J. Phys. Chem. Solids 23, 1381 (1962).
[18]J. Stöhr and J. D. Cashion, Phys. Rev. B 12, 4805 (1975).
[19]B. Bleany, Proc. R. Soc. A 276, 19 (1963).
[20]G. T. Trammel, Phys. Rev. 131, 932 (1963).
[21]J. H. Van Vleck, *The Theory of Magnetic Susceptibilities* (Oxford U.P., New York, 1932), p. 194.